

Stability Analysis of Steel Pipe Jacking under Combined Axial Pressure and Confining Pressure

Pengfei Chen^{1,*}, Chuhuai Xiao¹ and Jiang Li²

¹School of Architecture and Civil Engineering, Xi'an University of Science and Technology, Xi'an 710054, China

²China Railway 19th Bureau Group Company Limited, Beijing 100176, China

Received 2 January 2023; Accepted 27 March 2023

Abstract

During steel pipe jacking (SPJ), if improper control of jacking force or excessive water and earth pressure occurs, axial overall buckling and local buckling may happen. To reveal the stability mechanism of SPJ in the construction stage, cylindrical thin shell elastic stability theory was introduced. Theoretical analysis was used to derive the analytical equation of axial elastic buckling critical load under the combined action of uniform axial pressure and uniform confining pressure for engineering application. The finite element method was then employed to verify the analytical equation. Subsequently, the influence of pipe geometry parameters and uniform confining pressure on the axial buckling critical load was analyzed using the variable analysis method. The results show that: the analytical formula proposed in this study is in good agreement with the finite element calculation results; the critical load under the action of uniform axial pressure decreases with the increase of diameter-thickness ratio of the pipe when the slenderness ratio is less than 3; the critical load of axial buckling under different wall thickness decreases with the increase of uniform confining pressure, under the combined action of uniform axial pressure and uniform confining pressure; the thinner the wall thickness and the longer the pipe length, the greater the decrease of critical load; in actual construction, if the conditions allow, the axial stability of the SPJ can be improved by controlling the burial depth or wall thickness to avoid axial instability. This study provides a good reference for verifying whether the burial depth and wall thickness of a pipe meet the stability requirements.

Keywords: Steel pipe jacking, Uniform axial pressure, Uniform confining pressure, Combined action

1. Introduction

Pipe jacking is an important non-excavation pipeline construction technology, which is increasingly used in various underground pipeline projects. It is developing toward large diameter and long jacking distance, adapting to complex strata. The construction of pipe jacking method can be summarized as follows: using hydraulic jacks to jack the pipe sections in sequence from the starting well, while using manual excavation or mechanical excavation to discharge the soil until the receiving well, and finally forming a complete pipeline by effective connection between pipe sections [1]. After decades of using pipe jacking construction, plenty of practical experience has been accumulated in the design of construction equipment and technology. This includes construction equipment, from earth pressure balance tunneling machines to slurry pressure balance tunneling machines; key construction technologies, from manual excavation to mechanized excavation; slurry and intermediate jacking stations; and pipe materials, from reinforced concrete pipes and steel pipes to other types of composite material pipes [2].

The loading of steel pipe jacking (SPJ) during the construction phase is complex, mainly including the jacking the critical load of SPJ is an urgent problem to be solved.

Given the above analysis, this study derives the elastic

force, the resistance at the end, and the water and earth pressure exerted by the surrounding environment. As the diameter of the SPJ increases and the jacking distance grows, the jacking force must be increased. During jacking, if the jacking force is not properly controlled, axial overall instability may occur. Similarly, under the joint action of excessive surrounding stratigraphic water and earth pressure and axial jacking force, local and overall instability are likely to happen. This phenomenon is also confirmed by certain long-distance SPJ instability accidents [3].

Basing on this phenomenon, scholars conducted substantial research on the stability of SPJ in the construction phase. However, because the model established considers the situation in a relatively simple way, it cannot theoretically reveal the destabilization mechanism of SPJ [4-6]. Moreover, the construction method and loading conditions of SPJ differ from those of buried pipes, so the calculation of wall stability of buried flexible pipes in the code does not apply to SPJ [7]. Therefore, how to accurately reveal the destabilization mechanism of SPJ from the theoretical aspect and clarify the relationship between the geometric parameters of pipe jacking and burial depth and

stability equation of SPJ under composite load by introducing elastic stability theory and compares the theoretical results with the finite element calculation results. It aims to reveal the change law and influencing factors of elastic instability of SPJ more accurately.

*E-mail address: cpf125803@163.com

ISSN: 1791-2377 © 2023 School of Science, IHU. All rights reserved.

doi:10.25103/jestr.162.11

2. State of the art

The pipe of SPJ has a thin-walled cylindrical shell structure, of which steel is a typical elastoplastic material. The strength of this elastoplastic cylindrical shell structure is closely related not only to the strength of the material itself but also to the stability of the structure under consideration. The study of buckling instabilities in thin-walled cylindrical shell structures of steel pipes and other materials has become more mature. The classical theory of structural buckling was formed by Euler's pioneering study of the buckling of compressed rods in the mid-eighteenth century. Subsequently, the critical buckling solutions for cylindrical shells subjected to uniform axial and confining pressures were given by von Mises and Lorenz, among others [8]. Scholars conducted a number of studies on the sensitivity of cylindrical shell stability to structural nonlinearities and initial geometric defects [9]. Teng [10] analyzed the influence of different forms of initial defects such as welds and depressions as well as the diameter–thickness ratio (D/t) and internal pressure on the axial compression stability of cylindrical shells. The analysis showed that the presence of depressions at the welds was the form of defects that had the greatest influence on the stability of the structure. Omara [11] analyzed the pipe buckling problem caused by ellipticization, derived the expression for critical buckling pressure based on ellipticization, and verified the correctness of the analytical formula by the test of relevant pipe ellipticization. Zhu *et al.* [12] proposed an empirical formula for calculating the critical load of axially pressurized cylindrical shell buckling by analyzing a large amount of experimental data. Hiroyuki [13] studied the buckling problem of uniform isotropic cylindrical shell under axial pressure; analyzed the influences of shear deformation, wall thickness variation, and other factors on the higher order deformation of cylindrical shell; and compared the analytical results with existing theories.

Underground pipelines such as steel pipes were first laid by trenching and then backfilling and their stability problems were focused on pipeline deformation and instability caused by internal and external pressures. Research on buckling instability of underground pipes such as steel pipes has been more mature as well. For example, Palmer [14] first proposed the problem of buckling of buried pipes, i.e., the pipeline buckles due to the expansion of the pipe due to high internal pressure. Nazemi *et al.* [15] analyzed the process of buried pipes from the occurrence of local buckling to complete damage by full-scale tests and finite element verification for practical engineering problems. Murray [16] studied the local buckling and post buckling of buried pipes considered as cylindrical shell structure subjected to bending using experiments and combined with numerical simulations and further analyzed the force-deformation mechanism of buried pipes. Schaumann *et al.* [17] investigated the elasto-plastic buckling of steel buried pipe lines subjected to internal pressure and four-point bending as cylindrical shell structures. Ahmed *et al.* [18] established a finite element model to analyze the actual engineering and experimental phenomena and studied the local buckling and post-buckling behavior of steel buried pipes in cold regions considering material nonlinearity, large displacements, large rotations, initial defects, and complex contact surface conditions. Schneider [19] experimentally and theoretically studied the mechanical properties of buried all-welded pressure casing under internal pressure, axial

pressure, and four-point bending and established an analytical method that can quickly calculate the inelastic deformation strength of the pipe. The above study is mainly for the instability of the pipe subjected to internal pressure and external water and earth pressure and only applicable to the study of buried pipes.

Study results about the buckling instability of SPJ abound. Lu [20] conducted elastic-plastic analysis of large-diameter SPJ in soft ground section by theoretical calculation. The conclusion is that that the design wall thickness of SPJ is more sensitive to the change of deformation modulus value of soil around the pipe. Zhao [21-22] analyzed the internal forces and deformation of the SPJ by numerical simulation and concluded that the stability conditions of the cross-section of the SPJ are the main factors controlling the wall thickness. Zhao then derived the optimal wall thickness. However, only the confining pressure is considered in the above analysis, which is not consistent with the actual loading of the pipe jacking. With the rise of numerical simulation methods, plenty of research results are achieved in the study of SPJ stability using numerical calculation. For example, Chen *et al.* [23] simplified the complex force form of the pipe and studied the ultimate bearing capacity of long SPJ by numerical simulation, considering the force conditions with initial defects in the construction stage. Shao [24] analyzed the influencing factors and variation law of critical buckling stress under axial pressure by establishing a nonlinear finite element model of SPJ in homogeneous soil and proposed an empirical formula for axial stability coefficient of SPJ. In the study of nonlinear buckling of large-diameter SPJ, Jiang *et al.* [25] took the residual strain generated by concentrated force as the initial defect of SPJ due to external force and investigated the influence of local defects on the stability of SPJ by finite element method. They then proposed the optimization of wall thickness of SPJ by combining engineering examples and specification algorithm. Li *et al.* [26] analyzed the flexure of large-diameter thin-walled SPJ under jacking force by using finite element and the influence of initial defects, soil and water pressure, and other factors on the critical stress of SPJ. Jing *et al.* [27] used finite elements to establish a 3D solid model of large-diameter SPJ, analyzed the influence law of pipe geometric parameters and burial depth on the stability of pipe jacking, and proposed an empirical formula for the stability coefficient of large-diameter SPJ. Shao *et al.* [28-29] simplified the SPJ to Winkler beam, established and solved the energy equation of SPJ in homogeneous soil under the action of axial jacking force, and analyzed the variation law of axial overall stability coefficient of SPJ and the influencing factors. However, they did not consider local buckling.

The above studies mainly explored the elastic stability of SPJ in the construction stage by simplifying the force form of SPJ and by numerical simulation, but few relevant studies were done for the theoretical derivation. Therefore, in this study, the theory of elastic stability of cylindrical thin shell is introduced. The expression of axial compression elastic buckling load of cylindrical shell under the combined action of uniform axial pressure and uniform confining pressure is derived by establishing the displacement differential equation for deformation of cylindrical shell [30]. Finally, the stability of the SPJ under the combined action of uniform axial pressure and uniform confining pressure is investigated using the method of mutual verification between numerical and theoretical analyses. The influencing factors and change laws of the stability characteristics of the SPJ are analyzed.

The remainder of this study as follows. Section 3 introduces the theory of elastic stability of cylindrical shell and numerical analysis methods and derives the stability equations of cylindrical shell under the combined action of axial pressure and confining pressure. Section 4 analyzes the stability of SPJ under the combined action of confining pressure and axial pressure by theoretical calculation and numerical simulation and derives the influence law of different geometric parameters and uniform confining pressure on the critical load of SPJ in axial pressure. The last section summarizes the study and draws relevant conclusions.

3. Methodology

3.1 Stability theory of pipe jacking structure

3.1.1 Uniform axial pressure action

Experimental studies show that the frictional resistance of the pipeline during jacking is almost constant when a suitable slurry is used, so frictional resistance is not considered in the analysis of this study [31]. The SPJ reduces to a cylindrical shell subjected to a pressure P_{cr} in the axial direction, as shown in Figure 1. The critical load for axial pressure buckling of cylindrical shell can be expressed as Eq. (1):

$$\sigma_{cr} = \frac{Et^3}{12t(1-\nu^2)} \left(\frac{m^2\pi^2}{l^2} + \frac{E}{r^2D} \frac{l^2}{m^2\pi^2} \right) \quad (1)$$

where t represents wall thickness, r represents radius, l represents the length about cylindrical shell, m represents the number of half waves that occur when the shell wall is destabilized, E represents elasticity modulus, and ν represents Poisson's ratio. Usually, σ_{cr} is a function of $m\pi/l$, so the expression for the minimum value of σ_{cr} can be obtained as:

$$\sigma_{cr} = \frac{E}{\sqrt{3(1-\nu^2)}} \frac{t}{r} \quad (2)$$

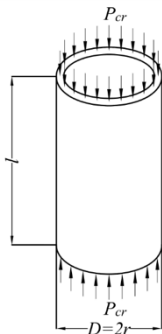


Fig. 1. Analytical model of cylindrical shell buckling under uniform axial pressure

3.1.2 Combined action of uniform axial pressure and uniform confining pressure

The cross-section of SPJ under water and earth pressure tend to produce elliptical deformation of vertical compression and horizontal stretch (as shown in Figure 2), which increases the lateral soil pressure of the pipe. Simultaneously, owing to the lighter self-weight caused by the unloading

rebound influence of the soil layer below, the distribution of water and earth pressure outside the pipe tends to homogenize. At this time, the soil pressure can be regarded as uniform confining pressure [23]. Thus, the SPJ reduces to a cylindrical shell under the combined action of uniform axial pressure P_{cr} and uniform confining pressure q , as shown in Figure 3.

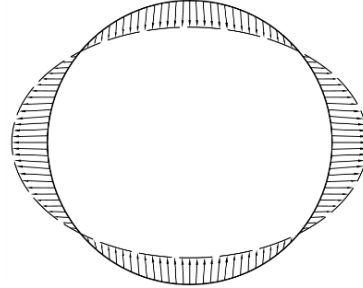


Fig. 2. Cross-sectional deformation of SPJ

Under the action of these forces, the shell may maintain its cylindrical shape. However, when the pressure drops to a certain critical value, the cylindrical shell may buckle and destabilize as the equilibrium form becomes unstable. With the help of elastic stability theory, the differential equations for the displacements u, v, w with respect to the deformation of the cylindrical shell are formulated (see Figure 4). By setting all the combined forces, N_x and N_y are expected to be small. Omitting the product of these forces with the derivative of the displacement u, v, w (they are also small), three equilibrium differential equations can be written to determine these displacements [30]. The following notation is used:

$$\frac{qr(1-\nu^2)}{Et} = \phi_1 \quad \text{and} \quad \frac{N_x(1-\nu^2)}{Et} = \phi_2 \quad (3)$$

These equilibrium differential equations are given as Eq. (4):

$$\begin{aligned} & r^2 \frac{\partial^2 u}{\partial x^2} + \frac{1+\nu}{2} r \frac{\partial^2 v}{\partial x \partial \theta} - \nu r \frac{\partial w}{\partial x} + r \phi_1 \left(\frac{\partial^2 v}{\partial x \partial \theta} - \frac{\partial w}{\partial x} \right) + \\ & + \frac{1-\nu}{2} \frac{\partial^2 u}{\partial \theta^2} = 0, \\ & \frac{1+\nu}{2} r \frac{\partial^2 u}{\partial x \partial \theta} + \frac{1-\nu}{2} r^2 \frac{\partial^2 v}{\partial x^2} + \frac{\partial^2 v}{\partial \theta^2} - \frac{\partial w}{\partial \theta} + \alpha \left[\frac{\partial^2 v}{\partial \theta^2} + \right. \\ & \left. + \frac{\partial^3 w}{\partial \theta^3} + r^2 \frac{\partial^2 w}{\partial x^2 \partial \theta} + \alpha^2 (1-\nu^2) \frac{\partial^2 v}{\partial x^2} \right] - r^2 \phi_2 \frac{\partial^2 v}{\partial x^2} = 0, \\ & \nu r \frac{\partial u}{\partial x} + \frac{\partial v}{\partial \theta} - w \alpha \left[\frac{\partial^3 v}{\partial \theta^3} + (2-\nu) r^2 \frac{\partial^3 v}{\partial x^2 \partial \theta} + r^4 \frac{\partial^4 w}{\partial x^4} \right. \\ & \left. + r^4 \frac{\partial^4 w}{\partial x^4} + \frac{\partial^4 w}{\partial x^4} + 2r^2 \frac{\partial^3 w}{\partial x^2 \partial \theta} \right] = \phi_1 \left(w + \frac{\partial^2 w}{\partial \theta^2} \right) + \\ & + \phi_2 r^2 \frac{\partial^2 w}{\partial x^2}. \end{aligned} \quad (4)$$

In Eq. (4), let u, v and w denote the small displacements about the cylindrical shell away from the position of the pressurized equilibrium form during buckling. Placing the

origin of the coordinates at one end of the shell, the form of the general solution about differential equation is:

$$\begin{aligned} u &= A \sin n\theta \cos \frac{m\pi x}{l}, \\ v &= B \cos n\theta \sin \frac{m\pi x}{l}, \\ w &= C \sin n\theta \sin \frac{m\pi x}{l}. \end{aligned} \quad (5)$$

Assume that the bus is divided into m half waves when the cylindrical shell flexes, whereas the circumference is divided into $2n$ half waves. At both ends, there are:

$$w = 0 \text{ and } \frac{\partial^2 w}{\partial x^2} = 0, \quad (6)$$

This is the condition for simply supported edges.

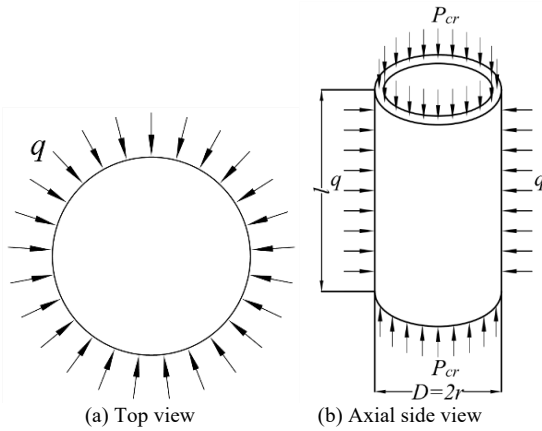


Fig. 3. Analytical model of cylindrical shell buckling under the combined influence of uniform axial pressure and uniform confining pressure

Substituting the general solution for the simple boundary condition into the differential Eq. (4), three homogeneous linear equations for A, B, C are obtained. The equations used to calculate the critical value of the pressure are proposed by setting the determinant of these equations equal to zero. After simplification, the formula is written as Eq. (7):

$$C_1 + C_2\alpha = C_3\phi_1 + C_4\phi_2, \quad (7)$$

The variables in Eq. (7) can be calculated through Eq. (8):

$$\begin{aligned} C_1 &= (1-\nu^2)\lambda^4, \\ C_2 &= (\lambda^2 + n^2)^4 - 2[\nu\lambda^6 + 3\lambda^4n^2 + (4-\nu)\lambda^2n^4 + n^6] + 2(2-\nu)\lambda^2n^2 + n^4, \\ C_3 &= n^2(\lambda^2 + n^2)^2 - (3\lambda^2n^2 + n^4), \\ C_4 &= \lambda^2(\lambda^2 + n^2)^2 + \lambda^2n^2, \\ \alpha &= \frac{t^2}{12r^2}; \lambda = \frac{m\pi r}{l}. \end{aligned} \quad (8)$$

From the equation, if the geometric parameters of the cylindrical shell are known and the number of axial as well as the circumferential half-wave is assumed, a certain linear relationship between ϕ_1 and ϕ_2 of the external pressure is

determined. In the pipe jacking construction, the uniform confining pressure on the outer wall about the pipe is relatively small compared with the axial force. To facilitate the calculation about critical load for the axial buckling of the pipe under different uniform confining pressures, Eq. (3) is substituted into Eq. (7) and deformed. The results are as follows:

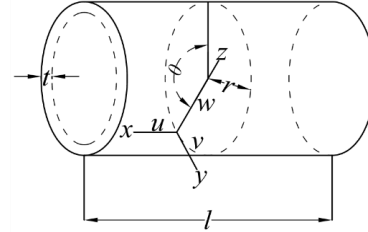


Fig. 4. Schematic diagram of cylindrical shell displacement

$$\sigma_{cr} = \frac{E(C_1 + C_2\alpha - C_3 \frac{qr(1-\nu^2)}{Et})}{C_4(1-\nu^2)} \quad (9)$$

By retaining the main term in Eq. (9), the simplified equation can be obtained as follows:

$$\begin{aligned} \sigma_{cr} &= \left\{ Et^3 \left[\left(\frac{\pi r}{l} \right)^2 + n^2 \right]^2 - 12r^3n^2q(1-\nu^2) \right\} / \\ &\left[\left[\left(\frac{\pi r}{l} \right)^4 + 2n^2 \left(\frac{\pi r}{l} \right)^2 \right] \times \left[\left(\frac{\pi r}{l} \right)^2 + n^2 \right]^2 \right. \\ &\left. + \frac{E}{1 + 2n^2 \left(\frac{l}{\pi r} \right)^2} \right] \end{aligned} \quad (10)$$

In the elastic phase, a linear relationship is observed between the axial buckling critical load of the SPJ and the confining pressure on the pipe, and it is related to the instability half-wave number and the geometric parameters of the SPJ. In the calculation, let equal to 2, 3, 4, 5, and substitute the geometric parameters. The minimum value is the pipe axial pressure buckling critical load under the action of different confining pressures.

3.2 Finite element analysis methods

In this study, eigenvalue buckling (buckle analysis step) in ABAQUS software is used to analyze the elastic stability of SPJ. The eigenvalue buckling analysis is a method that uses buckling theory to transform the load determination into a linear eigenvalue root solution, and its control equation [32] is:

$$(\mathbf{K}_0 + \lambda_i \mathbf{K}_\Delta) \mathbf{v}_i = 0 \quad (11)$$

where \mathbf{K}_0 denotes the substrate stiffness matrix, the influence of the applied load on the stiffness, \mathbf{K}_Δ is the stiffness matrix corresponding to the incremental load in the buckle analysis step, λ_i is the eigenvalue, and \mathbf{v}_i represents the eigenvalue vector about the i th eigenvalue corresponding to the buckling modes. The buckling load $p_{cr} = p_0 + \lambda_i p_\Delta$ of

the i th mode, where the minimum value of λ_i , is the most important. The method assumes perfect structural geometry and ideal material elasticity, and the results of the calculations are classical elastic theory solutions.

The ideal elastic model is used for the pipe material, with an elastic modulus $E=206Gpa$, Poisson's ratio $\nu=0.3$, and yield stress $\sigma_{cr}=235Mpa$. The geometric dimensions of the basic model are as follows: the outside diameter of the pipe is $D=3.6m$, the minimum wall thickness is $t=0.018m$, the maximum is $t=0.036m$, the grade difference is $0.002m$, and the length of the pipe section is $L/D=0.5,1,2,3$. In the calculation, the following assumptions are made:

- (1) Stability analysis is performed only on the steel pipe itself without considering the pipe soil interaction.
- (2) The self-weight influence of the SPJ is ignored.
- (3) Boundary condition: one end constrains the displacement in three directions, and the other end constrains the confining and radial displacement.

4. Result Analysis and Discussion

4.1 Theoretical calculations

4.1.1 Uniform axial pressure action

The selected pipe geometric parameters are as follows: pipe outside diameter $D=3.6m$, wall thickness taken as minimum $t=0.018m$, maximum $t=0.036m$, grade difference 2 mm , slenderness ratio $L/D=0.5,1,2,3$. They are substituted into Eq. (2) to calculate the cylindrical shell axial compression elastic buckling critical load. The calculated results are presented in Table 1. Figure 5 depicts the finite element calculation results of Section 4.2.1 and theoretical formula comparison results.

In Table 1, the wall thickness has a greater influence on the critical load of the pipe axial pressure, and the diameter–thickness ratio (D/t) increases by 20 for each. The maximum decrease in critical load is 40%, and the minimum decrease is 27%. In Figure 5, the critical load calculated by finite element calculations is closer to the exact solution of the theoretical equations, with an error range of 0.3% to 4%.

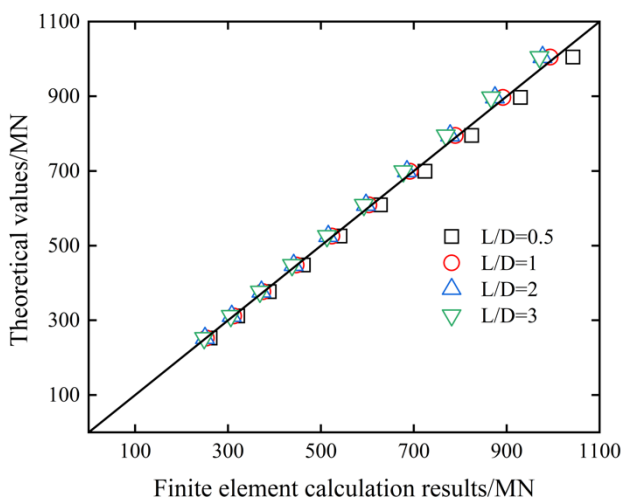


Fig. 5. Comparison about the finite element calculation results and theoretical formula

4.1.2 Combined action of uniform axial pressure and uniform confining pressure

The pipe geometric parameters are substituted into Eq. (10). The axial buckling critical loads under different confining pressures are obtained and compared with the calculation result of Section 4.2.2. The results are shown in Figures 6 and 7.

The influence of uniform confining pressure on the axial buckling critical load is shown in Figure 6 for different L/D and pipe wall thicknesses. The dependence of the uniform confining pressure on the axial buckling critical load is essentially linear, and the axial buckling critical load gradually decreases as the uniform confining pressure increases. When L/D is small, the axial buckling critical load at different wall thicknesses is less affected by the uniform confining pressure. The uniform confining pressure has a larger influence on the axial buckling critical load with respect to the SPJ when L/D is reduced, and the influence is larger for thinner wall thickness. At $L/D=0.5$ and 1, for every 50 kPa increase in the mean confining pressure, the reduction of axial buckling critical load for different wall thicknesses is within 5%. At $L/D=2$ and 3, the reduction of axial buckling critical load is the largest at a wall thickness of 18 mm, accounting for 26% and 35%, respectively. The smallest is at a wall thickness of 36 mm, which is within 3%. Figure 7 shows the results of comparing the calculated values of the finite elements with the theoretical equations. At $L/D=0.5$ and 1, the finite element values are in good agreement with the theoretical values. At $L/D=2$ and 3, the finite element values are in better agreement with the theoretical values when the wall thickness is thin and are lower than the theoretical values when the wall thickness is thick. In general, the finite element values of the axial buckling critical load under uniform confining pressure agree well with the theoretical values.

4.2 Numeric analysis

4.2.1 Uniform axial pressure action

The calculations are presented in Figures. 8 and 9 by imposing simple support boundary conditions on both ends of the steel pipe and setting a uniform axial pressure at the wall of the pipe at the end of the unconstrained axial displacement.

Figure 8 shows the influence of L/D on the axial buckling critical load, which shows that as L/D increases from 0.5 to 3, the axial buckling critical load shows essentially the same trend for different wall thicknesses, decreasing by 4% to 6%. Figure 9 shows the influence of L/D on axial buckling critical load, with the increase of D/t , the trend of axial buckling critical load for different L/Ds are basically the same, and the maximum decrease of critical load is 30% and the minimum decrease is 18% for every 20 increase of D/t .

Table 2. Theoretical values of the axial buckling critical load of cylindrical shell

Wall thickness /mm	18	20	22	24	26	28	30	32	34	36
Theoretical values /MN	51.15	70.09	93.19	120.85	153.48	191.47	235.24	285.18	341.67	405.13

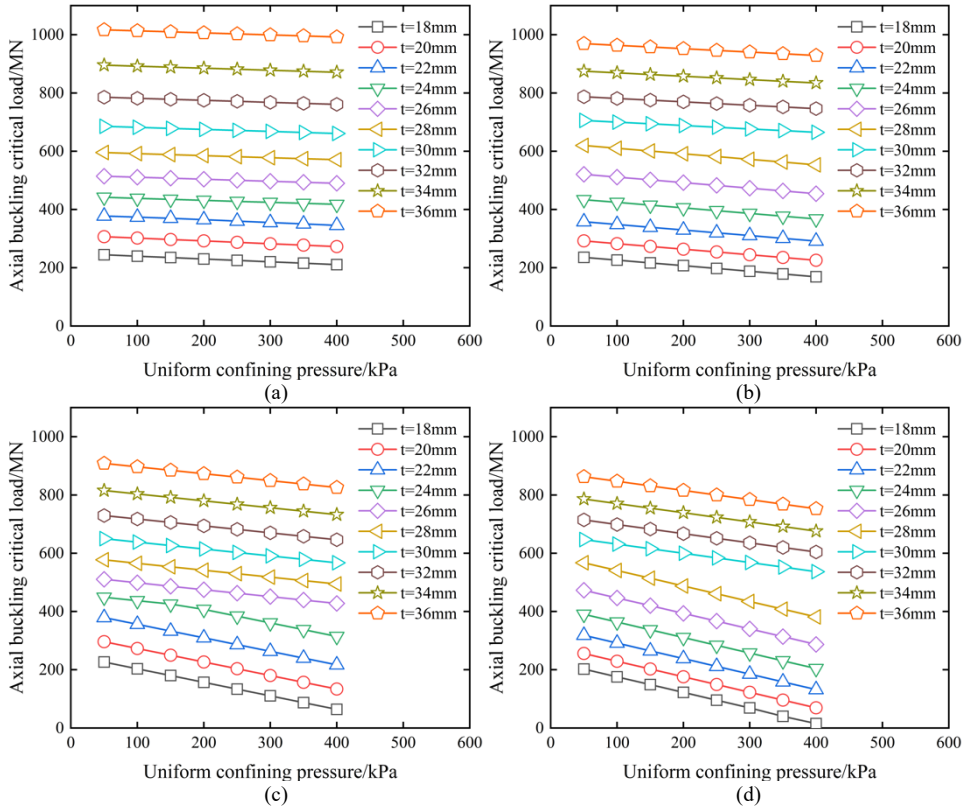


Fig. 6. Influence of uniform confining pressure on axial buckling critical load: (a) $L/D = 0.5$; (b) $L/D = 1$; (c) $L/D = 2$; (d) $L/D = 3$

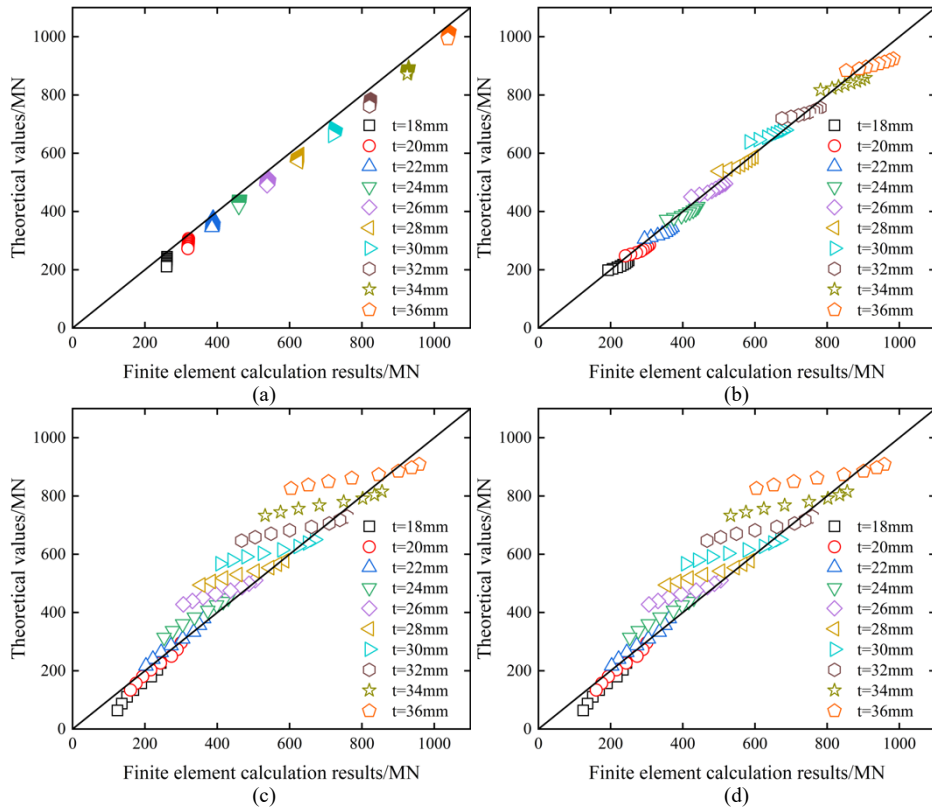


Fig. 7. Comparison of finite element calculation results and theoretical formula: (a) $L/D = 0.5$; (b) $L/D = 1$; (c) $L/D = 2$; (d) $L/D = 3$

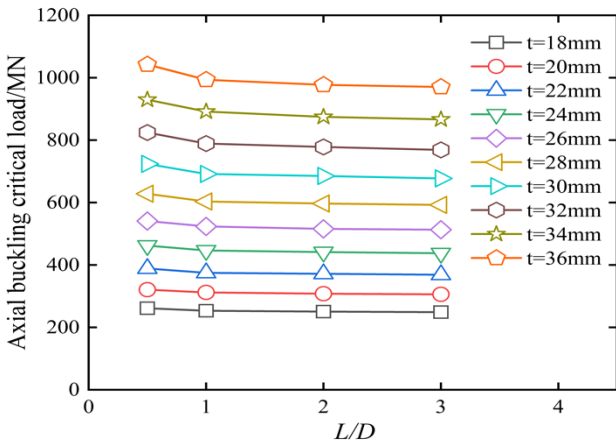


Fig. 8. Influence of slenderness ratio (L/D) on the critical load of axial compression elastic buckling

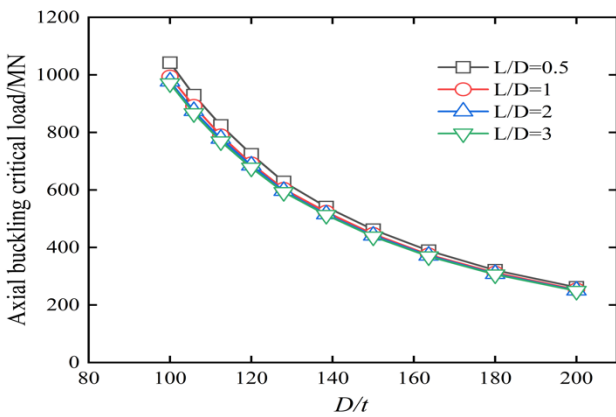


Fig. 9. Influence about diameter-thickness ratio (D/t) on the critical load about axial compression elastic buckling

4.2.2 Combined action of uniform axial pressure and uniform confining pressure

The axial pressure elastic buckling critical load of the pipe is solved using the above method, and the results are shown in Figure 10.

Figure 10 shows the influence of different confining pressures on the critical load for elastic buckling of the axial pressure of the pipe under the combined action of uniform confining pressure and uniform axial pressure. The critical load gradually decreases as the uniform confining pressure increases. At $L/D=0.5$ and 1, the uniform confining pressure has a small influence on the critical load. At $L/D=2$ and 3, the uniform confining pressure has a larger influence on the critical load, and the influence is larger for thinner walls of the pipe.

When the uniform confining pressure is increased from 50 kPa to 200 kPa, the critical load decreases within 6% for $L/D=0.5$ and 1. For $L/D=2$ and 3, the critical load decreases the most when the wall thickness is 18 mm, which is 22% and 37%, respectively, and the least is when the wall thickness is 36 mm, which is 11% and 20% respectively. When the mean confining pressure increases from 200 kPa to 400 kPa, the critical load of $L/D=0.5$ and 1 is reduced by 0.3% and 17%, respectively, when the wall thickness is 18mm. The critical load of $L/D=2$ and 3 is reduced the most when the wall thickness is 18 mm, which is 34% and 38%, respectively, and the least is when the wall thickness is 36 mm, which is 28% and 31%, respectively.

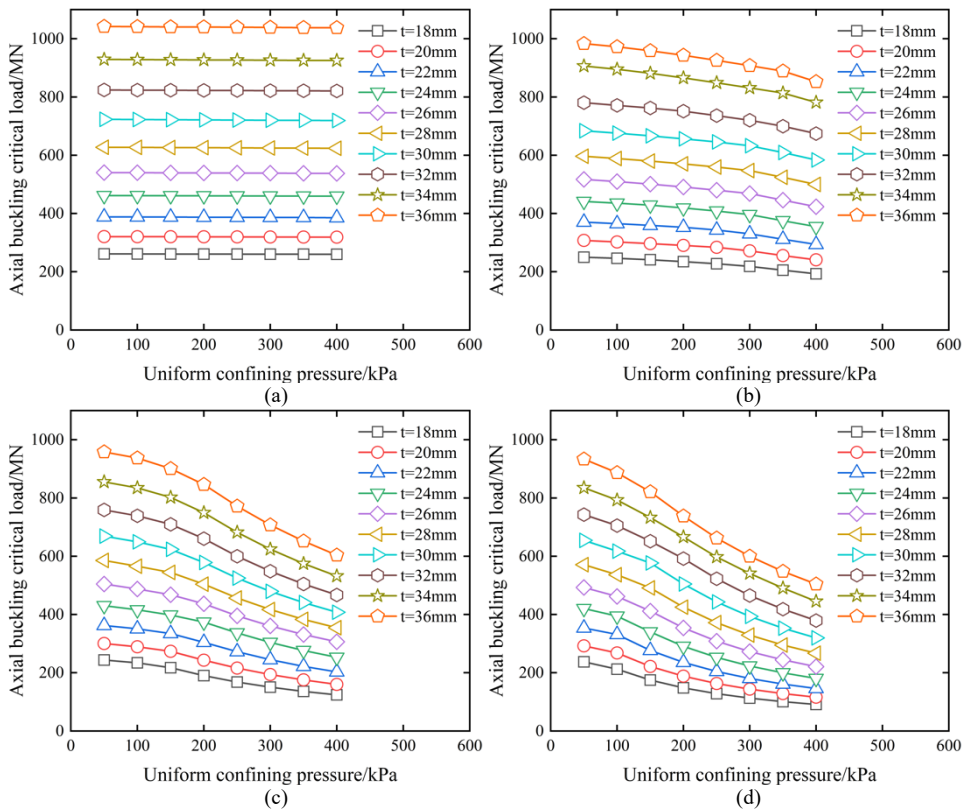


Fig. 10. Influence of uniform confining pressure on axial compression buckling critical load: (a) $L/D = 0.5$; (b) $L/D = 1$; (c) $L/D = 2$; (d) $L/D = 3$

4.3 Analysis of results

From the above calculation results, the critical load under the action of uniform axial pressure decreases with the increase of D/t when $L/D < 3$. The critical load under the combined action of uniform axial pressure and uniform confining pressure decreases with the increase of uniform confining pressure, and the influence of uniform confining pressure on the critical load is larger when the L/D is larger and the wall thickness is thinner.

In actual construction, the SPJ is usually buried at a depth of about 10 m to 12 m, and the vertical water and earth pressure of the pipe is estimated to be about 200 kPa [7]. From the calculation results in Sections 4.1.2 and 4.2.2, when the $L/D=3$, the uniform confining pressure increases from 50 kPa to 200 kPa, and the critical load is decreased by 37% at the maximum when the wall thickness $t=18\text{mm}$, and by 7% at the minimum when the wall thickness $t=36\text{mm}$. The minimum amplitude is 7%. When the mean confining pressure is increased from 200 kPa to 400 kPa, the critical load is reduced by 80% at the maximum wall thickness $t=18\text{mm}$ and 10% at the minimum wall thickness $t=36\text{mm}$.

When the uniform confining pressure is 200 kPa, it belongs to normal confining pressure, and the critical load of SPJ under the action of uniform confining pressure shows a small decrease. When the confining pressure is 400 kPa, it belongs to high confining pressure, and the critical load drops significantly when the pipe wall thickness is thin, and the maximum decrease can reach 80%. Therefore, in actual construction, if conditions allow, the burial depth can be reduced with respect to the pipe or increase the wall thickness to improve the axial stability of the SPJ and avoid axial instabilities.

5. Conclusions

To explore the stability of SPJ in the construction stage, a combination of theoretical derivation and numerical simulation is used to analyze the SPJ with different geometric parameters and different confining pressures. The conclusions are as follows:

(1) This study adopts a combination of numerical analysis and theoretical calculation to analyze the elastic stability characteristics of SPJ under uniform axial pressure and the combined action of uniform axial pressure and confining pressure. The calculation result shows that the theoretical values are concordant with the finite element values.

(2) The critical load under uniform axial pressure decreases with the increase of D/t when $L/D < 3$.

(3) The critical load under the combined action about uniform axial pressure and uniform confining pressure gradually decreases with the increase of uniform confining pressure. When the slenderness ratio is small ($L/D=0.5,1$), the axial buckling critical load with different wall thicknesses is less affected by the uniform confining pressure. When the slenderness ratio is large ($L/D=2,3$), the uniform confining pressure has a greater influence on the axial buckling critical load. The thinner the wall thickness, the greater the influence.

(4) In actual construction, if the conditions allow, the axial stabilities of SPJ can be enhanced by controlling the burial depth of the SPJ or the thickness of SPJ wall to avoid the occurrence of axial instability.

This study combines theoretical derivation and numerical simulation to propose the analytical equation of axial buckling critical load under the combined action of uniform confining pressure and uniform axial pressure. This approach is convenient for engineering verification of pipe burial depth and wall thickness and has reference significance for the stability design of pipe jacking construction. As the confining pressure is not completely uniformly distributed in the actual construction, the analytical equation for the axial pressure critical load must be derived under the combined action of non-uniform confining pressure and uniform axial pressure in future research. The understanding of the stability mechanism of SPJ in construction will then be more accurate.

This is an Open Access article distributed under the terms of the Creative Commons Attribution License.



References

- Chapman, D., Metje, N., Stärk, A., "Introduction to Tunnel Construction". London: Spon Press, UK, 2010, pp.123-128.
- Chapman, D., Rogers, C., Burd, H., Norris, P., Milligan, G., "Research needs for new construction using trenchless technologies". *Tunn Undergr Space Technol*, 22(5), 2007, pp.491-502.
- Zhen, L., Chen J.J., Qiao P.Z., et al. "Analysis and remedial treatment of a steel pipe-jacking accident in complex underground environment". *Engineering Structures*, 59, 2014, pp.210-219.
- Chen, B.Q., "Research on buckling deformation of steel pipe jacking in pipe jacking construction". *Municipal Technology*, 38(1), 2020, pp.104-107.
- Zhen, C., Ma B.S., "Analysis of steel pipe stability in pipe jacking construction based on ABAQUS". *Water Supply and Drainage*, 52(4), 2016, pp.99-103.
- Xuan, F., Huang, B., Xia, X., "Research on longitudinal stability of steel pipe jacking based on Pasternak foundation model". *Special Structure*, 37(1), 2020, pp.48-83.
- CECS 246-2008., "Technical specification for pipe jacking of water supply and sewerage engineering". Beijing: China Planning Press, China, 2008, pp.32-33.
- Chen, S., "Steel Structure Stability Design Guide". 3rd ed, Beijing: China Construction Industry Press, China, 2013, pp.369-382.
- Cui, D.G., "Structural Stability Design Manual". Beijing: Aviation Industry Press, China, 2006, pp.48-63.
- Teng, J.G., Rotter J.M., "Buckling of pressurized axisymmetrically imperfect cylinders under axial loads". *Journal of Engineering Mechanics*, ASCE, 118(2), 1992, pp.229-247.
- Omara, A., Guice, L.K., Straughan, W.T., Akl, F., "Instability of Thin Pipes Encased in Oval Rigid Cavity". *Journal of Engineering Mechanics*, 126(4), 2000, pp.381-388.
- Zhu, E., Mandal, P., Calladine, C.R., "Analysis of buckling thin cylindrical shells under axial compression". *Journal of Civil Engineering*, 34(3), 2001, pp.18-22.
- Hiroiyuki, M., "Buckling of Homogeneous Isotropic Cylindrical Shells under Axial Stress". *Journal of Engineering Mechanics*, 125(6), 1999, pp.613-621.
- Palmer, A.C., White, D.J., Baumgard, A.J., Bolton, M.D., Barefoot, A.J., Finch, M., Powell, T., Faranski, A.S., Baldry, J., "Uplift resistance of buried submarine pipelines: comparison between centrifuge modelling and full-scale tests". *Géotechnique*, 53(10), 2003, pp.877-883.
- Nazemi, N., Das, S., Kenno, S., "Finite element analysis for telescopic deformation and tearing rupture of wrinkled pipe". *International Journal of Offshore and Polar Engineering*, 19(3), 2009, pp.224-231.

16. Murray, D.W., "Local buckling, strain localization, wrinkling and postbuckling response of line pipe". *Engineering Structures*, 19(5), 1997, pp.360-371.
17. Schaumann, P., Keindorf, C., Bruggemann, H., "Elasto-Plastic Behavior and Buckling Analysis of Steel Pipelines Exposed to Internal Pressure and Additional Loads". *American Society of Mechanical Engineers*, 2005, pp.521-529.
18. Ahmed, A.U., Aydin, M., Cheng, J.J.R., Zhou, J., "Fracture of wrinkled pipes subjected to monotonic deformation: an experimental investigation". *Journal of Pressure Vessel Technology*, Transactions of the ASME, 133(1), 2011, pp.011401.
19. Schneider, S.P., "Flexural capacity of pressurized steel pipe". *Journal of Structural Engineering*, ASCE, 124(3), 1998, pp.330-340.
20. Lu, H.Q., "Elastoplastic analysis of large diameter steel pipe jacking on soft soil foundation and application". *Engineering Journal of Wuhan University*, 12(S1), 2009, pp.151-156.
21. Zhao, Z.F., Shao, G.H., "Stability analysis of wall stability of in pipe-jacking and optimization of proper wall thickness". *Engineering Journal of Wuhan University*, 44(4), 2011, pp.481-486.
22. Zhao, Z.F., Shao, G.H., "Three-dimensional numerical simulation of pipe jacking construction and optimization of steel pipe wall thickness". *Chinese Journal of Underground Space and Engineering*, 9(1), 2013, pp.161-165, 172.
23. Chen, N., "FEM analysis on the buckling of a long steel jacking pipe". *Journal of Shanghai Jiaotong University*, 46(5), 2012, pp.832-836.
24. Shao, G.H., Jiang Z.C., "Buckling analysis and stability coefficient study of large-diameter steel jacking construction". *Water Supply and Drainage*, 54(2), 2018, pp.94-98.
25. Jiang, Z.G., "Study on the optimization of the structure and the nonlinear buckling analysis of large-diameter steel jacking pipe". Master Thesis of Nanjing Forestry University, Nanjing, 2015, pp.55-59.
26. Li, Z.C., "Investigation on buckling mechanics of buried pipes". Master Thesis of Zhejiang University, Zhejiang, 2012, pp.65-69.
27. Jing, Z., Fang, P., Zhang, Y.Y., Li, W.J., "Stability of large diameter steel pipe jacking under the condition of high water level and weak stratum". *Science Technology and Engineering*, 22(27), 2022, pp.12131-12138.
28. Shao, G.H., Su, Y., Zhao, Z.F., "Energy method for stability of steel jacking pipes during construction in uniform soil". *Chinese Journal of Geotechnical Engineering*, 238(08), 016, pp.1490-1496.
29. Shao, G.H., Su, Y., Zhao, Z.F., "Allowable jacking force calculating method of steel jacking pipe considering axial deviation". *Chinese Journal of Underground Space and Engineering*, 14(03), 2018, pp.729-734.
30. Timoshenko, S.P., Gere, J.M., "Theory of elastic stability". Beijing: Science Press, China, 1961, pp.526-528. (translated by Zhang, F.F.)
31. Song, Z., Wan, Y., Huan, X., "Experimental study on the effect of injecting slurry inside a jacking pipe tunnel in silt stratum". *Tunnelling & Underground Space Technology*, 24(4), 2009, pp.466-471.
32. Li, J., "Buckling analysis of steel pipe jacking based on ABAQUS". *Urban Roads Bridges & Flood Control*, 284(12), 2022, pp.259-261, 30.